Frequency dependent complex resistivity inversion in 3D from Controlled-Source Electromagnetic data

J Porté, F Bretaudeau, J-F Girard

Frequency dependent complex resistivity inversion in 3D from Controlled-Source Electromagnetic data

J. Porté[3], F. Bretaudeau[1] and J-F. Girard[2]
[1]BRGM (French Geological Survey), f.bretaudeau@brgm.fr
[2]Strasbourg University, ITES-CNRS, UMR7063, France
[3]Formerly 1 2, now at SINTEF Industry, julien.porte@sintef.no

SUMMARY

In some rocks and soils, induced polarization (IP) phenomena are occurring when an electric perturbation is applied. These mechanisms are described by a *frequency dependent complex resistivity (CR)*. The study of relaxation model parameters describing these phenomena allows to access indirectly to several properties of interest of the underground, as properties linked to the pore space geometry, fluid content or presence and discrimination of disseminated metallic particles. Complex resistivity is usually studied using electrical method with a direct current hypothesis, in time or frequency domain. Electromagnetic induction coupling with the ground or cable layout are then neglected or considered as a source of noise, as they increase with frequency and larger offset. Thus, strong limitations appear to recover a complex resistivity image of buried target.
It leads several authors to rely on empirical EM induction retrieval techniques (Routh and Oldenburg, 2001) to manage IP data contaminated by EM effects. Lately, other authors worked to implement the problem of CR to Controlled-Source Electromagnetic method (CSEM), a resistivity imaging technique using multi-frequency electromagnetic signals fully taking into account EM induction. It uses thus the geometrical and the frequency sounding information of the ground for a larger investigation depth. Ghorbani et al (2009) developed, CR1Dinv, a 1D inversion code taking into account EM induction and IP effects for SIP data. Some codes at larger dimension exists but usually take into account only a constant complex resistivity as the work of (MacLennan et al, 2014) in 2.5D. Nevertheless, there still are a strong need of a method able to manage both effects in this domain. In this work, we implemented frequency dependent complex resistivity inversion in POLYEM3D, a 3D finite-difference modelling and inversion code for controlled-source electromagnetic data (CSEM) (Bretaudeau et al, 2021) in order to fully recover IP information contained in EM data. Through a three layers synthetic example, we present the inversion method developed to constrain the multi-parameters problem using an 1D inversion module fully implemented to the 3D code for methodological developments. Secondly, a 3D synthetic example is showed to illustrate a transposition of the developed inversion method to the 3D code.

Keywords: CSEM, complex resistivity, 3D inversion

METHOD

Frequency dependent CR implementation to the inversion problem leads to the multiplication of the number of parameters and so, to the number of equivalent solution. In order to constrain efficiently the multi-parameters problem, we decomposed the inversion through a multi-stages strategy. Indeed, the problem is decomposed in a two stages procedure, based on the electrical field sensitivity to CR. In a first stage, the resistivity norm $|\rho^*|$ is solved inverting the amplitude of the electrical field response which present a low sensitivity to the CR phase ϕ_{cpx} (1). From the retrieved model in the first stage, we invert in a second stage the electric field phase residual to obtain the CR phase ϕ_{cpx} image.

Furthermore, to manage the increasing number of parameters several empirical relaxation models are commonly used to describe CR spectrum, as the most used one, the Cole-Cole (CC) resistivity model (Cole and Cole, 1941)(Pelton et al, 1978). In this study, we chose to keep a general formulation of

the frequency dependent CR by using a $2^n d$ order polynomial parameterization. CR norm $|\rho^*|(\omega)$ and phase ϕ_{cpx} are the n parameters according to following equations :

$$|\rho^*(\omega)| \propto \mathcal{P}_2\omega^2 + \mathcal{P}_1\omega^1 + \mathcal{P}_0 \quad (1)$$

$$\Phi_{cpx}(\omega) \propto \mathcal{Q}_2\omega^2 + \mathcal{Q}_1\omega^1 + \mathcal{Q}_0 \quad (2)$$

The inversion problem is then reduced to 6 parameters per cell independently to the number of frequency used. In the multi-stages procedure describes above, only 3 parameters per cell are solved simultaneously. Method was developed using a 1D inversion module based on the semi-analytic solution forward code used to solve the primary electrical field of the 3D code and a gradient solved by perturbation. The optimisation is based on a Gauss-Newton estimation of the model update and a linesearch based on a bracketing strategy (Métivier and Brossier, 2016). In following example, we minimize the L2 norm of the logarithm of the data augmented by a Tikhonov regularisation with a maximum smoothness constrain (Grayver et al, 2013).

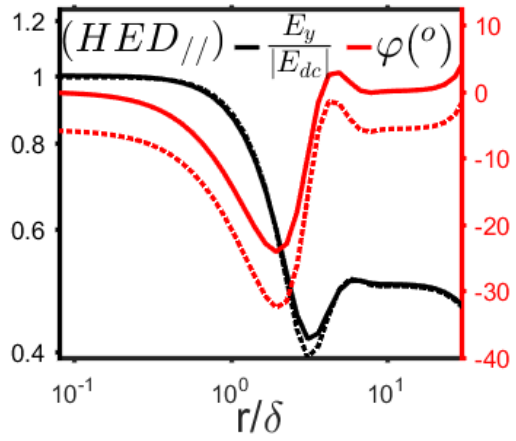

Figure 1: Normalized amplitude and phase of the electric response relative to the offset/skin depth δ ratio over a constant resistivity half-space with (dotted) and without (solid) -100 mrad of CR phase

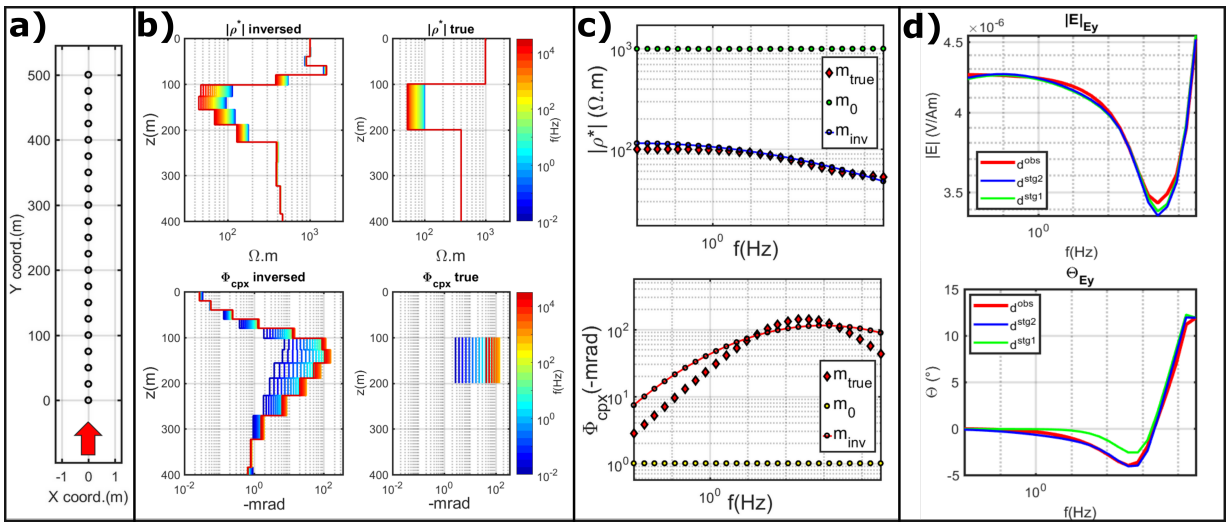

Figure 2: 1D inversion results (Gauss-Newton optimization and L2 norm) for a three layers synthetic model including a conductive polarizable layer accordingly to a Cole-Cole model ($\rho_0 = 100\Omega.m$ $m = 0.5$ $\tau = 0.001s$ $c = 0.5$). Final data $rms < 1\%$. a) Acquisition geometry using a horizontal electric dipole (HED) (red arrow); b) Inverted and true CR model sounding at each frequency (color lines); c) CR spectrum in the cell layer at z=150m for the starting model m_0, the true model m_{true} and the resulting model m_{inv}; d) Data fit (Electrical amplitude (top); Electrical phase (bottom)) at the station $y = 250m$: observed data in red, inverted data at end of stage 1 in green and the final data fit at end of stage 2 in blue

COMPLEX RESISTIVITY INVERSION RESULTS

Figure 2 presents the results from an 1D synthetic three layers model using our inversion strategy in 2 stages and a 2^{nd} order polynomial parametrization of CR. The second layer is a 100 meters conductive and polarizable layer according to a CC relaxation

model (ρ_0= 10 $.m$; m= 0.5; τ= 0.001 s; c = 0.5). We used inline electric field of an 500 meters acquisition profile with a 25 meters spacing, from an inline horizontal electric dipole (HED). 25 frequencies spaced logarithmically from 0.01 Hz to 30 kHz were used and starting model as a constant homogeneous half-space of $500\Omega.m$ and a CR phase of $-1mrad$.

Figure 2 b) shows CR soundings results at each frequency compared to the true CR model. The CR norm image is the result of the first stage whereas the CR phase image the result from the second stage of our inversion procedure. The layer geometry is well defined for $|\rho^*|$ and ϕ_{cpx} and the shape of the CR spectrum is correctly retrieved in the layer as shown in c). The data fit after each stage can be seen in d) for one of the reception sites. We can notice the residual remaining after stage 1 on the electrical phase being fitted in stage 2, without alterring significantly the fit on the amplitude.

Following the 1D development phase and previous results, the method was transposed to the 3D case in the main code POLYEM3D. l-BFGS optimization is used here. Gradient was computed using the adjoint-state method (Plessix and Mulder, 2008) for the CR case and appropriate change of variables were implemented in order to properly precondition the inverse problem and compensate the sensitivity heterogeneity. Figure 4 presents the results obtained for a simple 3D CR synthetic model inversion with a conductive and polarizable cube according to a CC model within a constant half-space with negligible CR phase ($100\Omega.m$ and $-1mrad$).

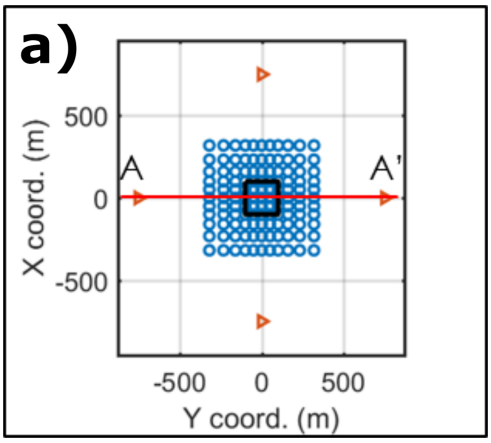

Figure 3: Surface acquisition geometry using 4 HED transmitters oriented to the center of a reception grid measuring the electrical field response (blue circles);

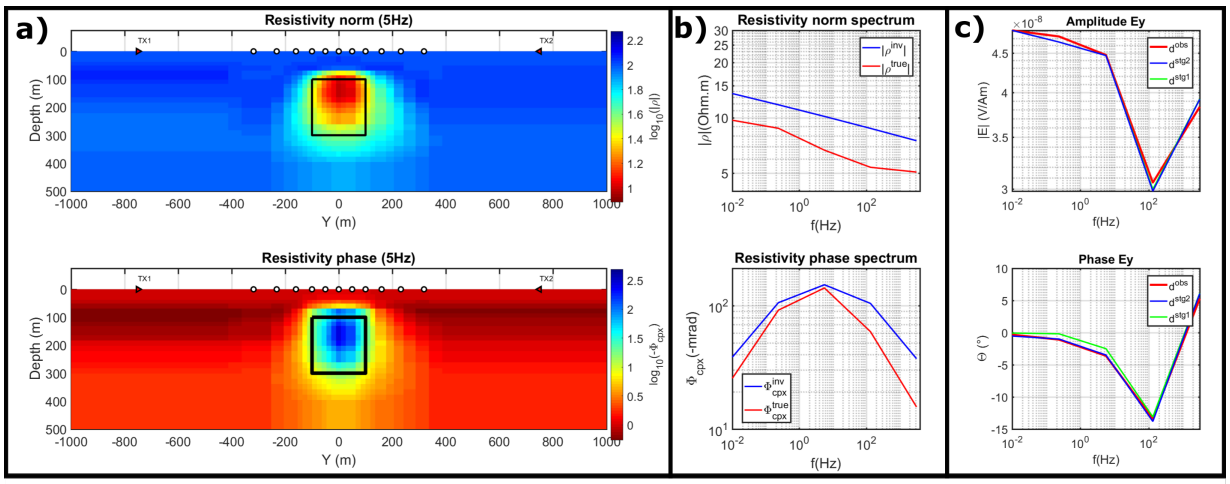

Figure 4: Results of the 3D inversion (l-BFGS optimization and L2 norm) of a polarizable cube (black square) accordingly to a Cole-Cole model ($\rho_0 = 10\Omega.m$ $m = 0.5$ $\tau = 0.1s$ $c = 0.5$) in a homogeneous background ($100\Omega.m$ and $-1mrad$). Final data $rms < 1\%$. b) Norm and phase image of the CR at 5 Hz extracted for the profile AA' in figure 3 . c) CR spectrum at the top-center of the cube ; d) Data fit at the reception site directly above the center of the cube

CONCLUSIONS

We show through 1D synthetic data inversions and preliminary 3D results that we are able to estimate a complex resistivity and its frequency variation from CSEM data by considering all the IP/EM coupling, when IP signals are sufficiently large compared to

EM induction. Our inversion strategy allows then to access to IP parameters of the medium in an extended frequency domain as well as for greater depth of investigation. A 3D CSEM survey was undertaken in December 2020 on the former mining site of La Porte-Aux-Moines (CÃ´tes-d'Armor, France) presenting strong IP responses, to validate our inversion method for a 3D in-situ dataset.

ACKNOWLEDGEMENTS

The research leading to these results has received fundings from the french ANR in the framework of projects EXCITING. Large scale modeling and inversion was performed using the CINES (Centre Informatique National de lâEnseignement SupÃ©rieur) supercomputer OCCIGEN.

REFERENCES

Bretaudeau F, Dubois F, Bissavetsy Kassa S, Coppo N, Wawrzyniak P, Darnet M (2021) Time-lapse resistivity imaging: Csem-data 3-d double-difference inversion and application to the reykjanes geothermal field. Geophysical Journal International 226(3):1764–1782

Cole KS, Cole RH (1941) Dispersion and Absorption in Dielectrics I. Alternating Current Characteristics. The Journal of Chemical Physics 9(4):341–351, DOI 10.1063/1.1750906, URL https://aip.scitation.org/doi/abs/10.1063/1.1750906, publisher: American Institute of Physics

Ghorbani A, Cosenza P, Revil A, Zamora M, Schmutz M, Florsch N, Jougnot D (2009) Non-invasive monitoring of water content and textural changes in clay-rocks using spectral induced polarization: A laboratory investigation. Applied Clay Science 43(3-4):493–502

Grayver AV, Streich R, Ritter O (2013) Three-dimensional parallel distributed inversion of CSEM data using a direct forward solver. Geophysical Journal International 193(3):1432–1446

MacLennan K, Karaoulis M, Revil A (2014) Complex conductivity tomography using low-frequency crosswell electromagnetic data. Geophysics 79(1):E23–E38

Métivier L, Brossier R (2016) The seiscope optimization toolbox: A large-scale nonlinear optimization library based on reverse communication-the seiscope optimization toolbox. Geophysics 81(2):F1–F15

Pelton WH, Ward SH, Hallof PG, Sill WR, Nelson PH (1978) Mineral discrimination and removal of inductive coupling with multifrequency IP. Geophysics 43(3):588–609

Plessix RE, Mulder W (2008) Resistivity imaging with controlled-source electromagnetic data: depth and data weighting. Inverse problems 24(3):034012

Routh PS, Oldenburg DW (2001) Electromagnetic coupling in frequency-domain induced polarization data: A method for removal. Geophysical Journal International 145(1):59–76